Journal of Computational Physics 328 (2017) 86–94

Contents lists available at ScienceDirect

Journal of Computational Physics

www.elsevier.com/locate/jcp

Short note

# Explicit Runge–Kutta schemes for incompressible flow with improved energy-conservation properties

F. Capuano [a,*], G. Coppola [a], L. Rández [b], L. de Luca [a]

[a] Dipartimento di Ingegneria Industriale (DII), Università di Napoli "Federico II", Napoli, 80125, Italy
[b] IUMA - Departamento de Matemática Aplicada, Universidad de Zaragoza, Zaragoza, 50009, Spain

ARTICLE INFO

*Article history:*
Received 15 February 2016
Received in revised form 1 September 2016
Accepted 14 October 2016
Available online 19 October 2016

*Keywords:*
Energy conservation
Incompressible Navier–Stokes equations
Runge–Kutta method
Pseudo-symplecticity
Turbulence simulations

ABSTRACT

The application of *pseudo-symplectic* Runge–Kutta methods to the incompressible Navier–Stokes equations is discussed in this work. In contrast to fully energy-conserving, implicit methods, these are explicit schemes of order $p$ that preserve kinetic energy to order $q$, with $q > p$. Use of explicit methods with improved energy-conservation properties is appealing for convection-dominated problems, especially in case of direct and large-eddy simulation of turbulent flows. A number of pseudo-symplectic methods are constructed for application to the incompressible Navier–Stokes equations and compared in terms of accuracy and efficiency by means of numerical simulations.



## 1. Introduction

Discrete conservation of kinetic energy is an important requirement in the numerical solution of the incompressible Navier–Stokes equations. In the inviscid limit, the global kinetic energy $e = \int_\Omega u_i^2/2\,\mathrm{d}V$ (i.e. the kinetic energy integrated over the domain $\Omega$) is an invariant of the continuous equations when periodic or homogeneous boundary conditions are applied [1]. The reproduction of this property on a discrete level is especially important when dealing with turbulent flow simulations, in the framework of either Direct (DNS) or Large-Eddy Simulation (LES) techniques. Enforcing discrete conservation of kinetic energy can lead to a number of desirable features, such as zero or negligible artificial dissipation, a well represented energy transfer mechanism as well as a nonlinear stability bound to the numerical solution [2–4].

The Navier–Stokes equations are usually tackled numerically by means of a semi-discrete approach, in which the various terms are first discretized in space and then integrated in time. In general, both the space discretization and time advancement algorithms contribute to violation of the discrete conservation of kinetic energy in the inviscid limit [5]. While various methods are available to accomplish spatial conservation, only a limited class of numerical algorithms can provide this property for the time-advancement step. These methods are necessarily implicit [6], and the application of fully implicit schemes to the Navier–Stokes equations presents several drawbacks. It is computationally expensive, especially when managing very large systems, and it is difficult to be carried out efficiently for massively parallel architectures. Explicit methods with optimal energy-preserving properties are thus warranted.

In this short note, the use of *pseudo-symplectic* Runge–Kutta (RK) schemes for time-integration of the Navier–Stokes equations is investigated. These are explicit methods that preserve quadratic invariants approximately up to a certain order

* Corresponding author.
*E-mail address:* francesco.capuano@unina.it (F. Capuano).

http://dx.doi.org/10.1016/j.jcp.2016.10.040
0021-9991/

of accuracy, and were introduced in the context of Hamiltonian systems [7,8]. The application of such schemes to the fluid flow equations is appealing and appears to have never been pursued in the available literature. Existing as well as newly derived pseudo-symplectic methods are constructed and optimized for application to the Navier–Stokes equations.

The short note is organized as follows. Details about the spatial and temporal discretization are briefly recalled in Section 2. Newly derived as well as existing pseudo-symplectic schemes are presented in Section 3. The performances of three selected methods are discussed in Section 4 by means of numerical tests. Concluding remarks are given in Section 5.

## 2. Spatial and temporal discretizations

The incompressible Navier–Stokes equations in Cartesian coordinates read:

$$\frac{\partial u_i}{\partial t} + \frac{\partial u_j u_i}{\partial x_j} = -\frac{\partial p}{\partial x_i} + \frac{1}{\mathrm{Re}} \frac{\partial^2 u_i}{\partial x_j \partial x_j}, \tag{1}$$

$$\frac{\partial u_i}{\partial x_i} = 0, \tag{2}$$

where summation over repeated indices is assumed. In the framework of finite-difference or finite-volume methods, a semi-discrete version of Eqs. (1–2) can be expressed as

$$\frac{\mathrm{d}\mathbf{u}}{\mathrm{d}t} + \mathbf{C}(\mathbf{u})\mathbf{u} = -\mathbf{G}\mathbf{p} + \frac{1}{\mathrm{Re}}\mathbf{L}\mathbf{u}, \tag{3}$$

$$\mathbf{M}\mathbf{u} = \mathbf{0}, \tag{4}$$

where $\mathbf{u}$ is the discrete velocity vector containing the three components on the three-dimensional mesh, $\mathbf{u} = \left[\mathbf{u}_x\, \mathbf{u}_y\, \mathbf{u}_z\right]^T$, the matrices $\mathbf{G} \in R^{N_\mathbf{u} \times N_p}$ and $\mathbf{M} \in R^{N_p \times N_\mathbf{u}}$ are the discrete gradient and divergence operators, respectively, while $\mathbf{L} \in R^{N_\mathbf{u} \times N_\mathbf{u}}$ is the block-diagonal Laplacian operator. The convective term is expressed as the product of a linear convective operator $\mathbf{C}(\mathbf{u})$ and $\mathbf{u}$. The specific forms of the operators $\mathbf{C}$, $\mathbf{L}$, $\mathbf{G}$ and $\mathbf{M}$ depend upon the details of the discretization scheme. For the sake of simplicity, equally spaced Cartesian grids will be considered in the following. This hypothesis does not prevent the generality and can be easily extended by considering a relevant inner product. It will also be assumed that the differential operators are discretized consistently, e.g. $\mathbf{G}^T = -\mathbf{M}$. Note that the index-2 Differential Algebraic Equation (DAE) system of Eqs. (3–4) can be recast concisely by enforcing the incompressibility constraint through the solution of the pressure Poisson equation [9]. Substitution of the constraint leads to the ODE system

$$\frac{\mathrm{d}\mathbf{u}}{\mathrm{d}t} = \mathbf{P}\mathbf{F}(\mathbf{u})\,\mathbf{u}, \tag{5}$$

where $\mathbf{F} = -\mathbf{C}(\mathbf{u}) + \frac{1}{\mathrm{Re}}\mathbf{L}$ and the projection operator $\mathbf{P} = \mathbf{I} - \mathbf{G}\mathcal{L}^{-1}\mathbf{M}$, with $\mathcal{L} = \mathbf{M}\mathbf{G}$, has been introduced.

This work is focused on the evolution of discrete kinetic energy. A global kinetic energy is defined as $E = \mathbf{u}^T\mathbf{u}/2$, and its semi-discrete evolution equation reads

$$\frac{\mathrm{d}E}{\mathrm{d}t} = -\mathbf{u}^T\mathbf{C}(\mathbf{u})\mathbf{u} - \mathbf{u}^T\mathbf{G}\mathbf{p} + \frac{1}{\mathrm{Re}}\mathbf{u}^T\mathbf{L}\mathbf{u}. \tag{6}$$

In Eq. (6), the only physical contribution is due to the diffusive term, that correctly dissipates energy since $\mathbf{L}$ is a negative-definite matrix. The pressure gradient contribution vanishes if $\mathbf{G}^T = -\mathbf{M}$ and $\mathbf{M}\mathbf{u} = 0$. It is useful to recall that this is true for *regular* or *staggered* arrangements of flow variables (using the terminology given in [10]), whereas pressure can contribute to the kinetic energy balance in *collocated* layouts as an error of order $\mathcal{O}(\Delta t^2 \Delta x^2)$ [11]. The convective term preserves energy if a skew-symmetric operator is adopted [12]. This property can be achieved in various ways; most notably, one can either discretize the so-called *skew-symmetric form* of convection [13], or adopt a proper staggered arrangement for the flow variables, with the convective term discretized in conservative formulation [14,10]. In the latter case, simultaneous enforcement of discrete mass conservation is required. In this work, discretely energy-conserving spatial schemes will be employed. In such cases, Eq. (5) forms a system of ODE possessing global kinetic energy as a quadratic invariant, for $\mathrm{Re} \to \infty$.

This short note is focused on numerical methods that are capable of preserving energy also for the time-advancement step. In general, time integration schemes do not preserve the quadratic invariants of the continuous system of ODE. While all RK and linear multistep methods preserve linear invariants [15], multistep schemes do not preserve quadratic invariants, while this is possible for some special implicit Runge–Kutta methods.

A general $s$-stage Runge–Kutta method applied to Eq. (5) can be expressed as

$$\mathbf{u}^{n+1} = \mathbf{u}^n + \Delta t \sum_{i=1}^{s} b_i \widetilde{\mathbf{F}}(\mathbf{u}_i)\mathbf{u}_i \tag{7}$$

$$\mathbf{u}_i = \mathbf{u}^n + \Delta t \sum_{j=1}^{s} a_{ij} \widetilde{\mathbf{F}}(\mathbf{u}_j)\mathbf{u}_j, \tag{8}$$

where $a_{ij}$ and $b_i$ are the RK coefficients and $\widetilde{\mathbf{F}} = \mathbf{PF}$. The RK methods are usually constructed to maximize the temporal order of accuracy of the method, hereinafter referred to as *classical* order $p$ (or simply order), in contrast to *pseudo-symplectic* order $q$, that will be introduced in the following section.

## 3. Pseudo-symplectic Runge–Kutta methods for Navier–Stokes equations

### 3.1. Energy analysis and order conditions

The energy-conservation properties of a Runge–Kutta method can be analyzed by deriving an expression for the kinetic energy variation introduced by Eqs. (7–8). The fully discrete evolution equation can be obtained in closed form by taking the inner product between $\mathbf{u}^{n+1}$ and itself. After some basic manipulation, one has

$$\frac{\Delta E}{\Delta t} = \frac{1}{\mathrm{Re}} \sum_i b_i \mathbf{u}_i^T \mathbf{L} \mathbf{u}_i - \frac{\Delta t}{2} \sum_{i,j=1}^{s} \left( b_i a_{ij} + b_j a_{ji} - b_i b_j \right) \mathbf{u}_i^T \widetilde{\mathbf{F}}^T (\mathbf{u}_i) \widetilde{\mathbf{F}} (\mathbf{u}_j) \mathbf{u}_j, \tag{9}$$

where $\Delta E = E^{n+1} - E^n$. Note that Eq. (9) in various different forms has been derived in [3,16,17], among others. Equation (9) is the discrete counterpart of the continuous kinetic energy equation

$$\frac{\Delta e}{\Delta t} = -\frac{1}{\mathrm{Re}} \frac{1}{\Delta t} \int_t^{t+\Delta t} \phi \, \mathrm{d}t, \tag{10}$$

where $\phi = \int_\Omega 2 S_{ij} S_{ij} \, \mathrm{d}V$ is the scalar dissipation function, and $S_{ij}$ is the symmetric part of the velocity gradient. Equation (9) differs from Eq. (10) due to the presence of the second term on the right-hand side, that represents the temporal error. The use of a spatial scheme that does not conserve kinetic energy would lead to an additional constant error term in Eq. (9).

Energy-conserving Runge–Kutta methods possess the following property:

$$b_i a_{ij} + b_j a_{ji} - b_i b_j = 0 \qquad \forall \, i, j = 1, \ldots, s. \tag{11}$$

The fulfillment of the above conditions allows to preserve the global kinetic energy (for inviscid flows), or to enforce the correct discrete kinetic energy balance (for viscous flows). In other words, it ensures that the variation of kinetic energy is solely due to the physical viscous dissipation. Equation (11) can only be satisfied by implicit methods. Therefore, a nonlinear system has to be solved to advance in a single time step, leading to implementation issues and remarkable computational effort [16]. Note that Eq. (11) can be shown to provide conservation of all quadratic invariants (including kinetic energy), and, for irreducible RK methods, is also a necessary and sufficient condition for *symplecticity* [6].

In the present work explicit schemes are considered, which are often preferred for turbulent flows simulations. In this case, the matrix of the $a_{ij}$ coefficients is lower triangular, i.e., $a_{ij} = 0$ for $j \geq i$. In the present context, an explicit method is said to be of *pseudo-symplectic order* $q$ if (and only if), for $\mathrm{Re} \to \infty$,

$$\frac{\Delta E}{\Delta t} = \mathcal{O}\left( \Delta t^q \right). \tag{12}$$

While in classical explicit methods one generally has $p = q = s$, in pseudo-symplectic methods the coefficients are constructed to satisfy additional conditions such that the error term in Eq. (9) is of order $q > p$. The pseudo-symplectic order conditions have been obtained by Aubry & Chartier [7] by employing the theory of trees; they are reported in Table 2.1 of the same work up to sixth order. The order conditions can be equivalently obtained by expanding Eq. (9) as a Taylor series in the time increment $\Delta t$. By using the linearity of the convective operator $\mathbf{C}(\mathbf{u}_i)$ and plugging Eqs. (7–8) into Eq. (9), one obtains

$$\begin{aligned} \frac{\Delta E}{\Delta t} = & -\Delta t \left[ C_2 \sum_{ij} g_{ij} \right] - \Delta t^2 \left[ C_3 \sum_{ijk} g_{ij} a_{jk} \right] - \Delta t^3 \left[ C_{4,1} \sum_{ijkl} g_{ij} a_{ik} a_{kl} + C_{4,2} \sum_{ijkl} g_{ij} a_{ik} a_{jl} \right] + \\ & - \Delta t^4 \left[ C_{5,1} \sum_{ijklm} g_{ij} a_{ik} a_{jl} a_{jm} + C_{5,2} \sum_{ijklm} g_{ij} a_{jk} a_{kl} a_{im} + C_{5,3} \sum_{ijklm} g_{ij} a_{jk} a_{kl} a_{jm} + \right. \\ & \left. + C_{5,4} \sum_{ijklm} g_{ij} a_{jk} a_{kl} a_{km} + C_{5,5} \sum_{ijklm} g_{ij} a_{jk} a_{kl} a_{im} \right] + \mathcal{O}(\Delta t^5), \end{aligned} \tag{13}$$

where $g_{ij} = b_i a_{ij} + b_j a_{ji} - b_i b_j$. The various coefficients $C$ are scalar functions that can be expressed as combinations of the convective operator. For further details about the derivation of Eq. (13), the reader is referred to [3,5].

The pseudo-symplectic order conditions can be easily obtained by nullifying the single independent terms in Eq. (13), and can be shown to be equivalent to those presented in [7]. They are reported here for convenience in Table 1, both in summation and vector notation.

**Table 1**
Pseudo-symplectic order conditions up to $q = 5$. The . operator represents pointwise multiplication, while $\mathbf{e} = (1, \ldots, 1) \in \mathbb{R}^s$. Also, $\mathbf{b} = b_i$, $\mathbf{A} = a_{ij}$, $\mathbf{c} = \mathbf{Ae}$.

| $q$ | Summation | Vector |
|---|---|---|
| 1 | $\sum_i b_i = 1$ | $\mathbf{b}^T\mathbf{e} = 1$ |
| 2 | $\sum_{ij} g_{ij} = 0$ | $\mathbf{b}^T\mathbf{Ae} + \mathbf{b}^T\mathbf{c} = \mathbf{b}^T\mathbf{e}$ |
| 3 | $\sum_{ijk} g_{ij}a_{jk} = 0$ | $\mathbf{b}^T\mathbf{Ac} + \mathbf{b}^T\mathbf{c}^2 = \mathbf{b}^T\mathbf{c} = 0$ |
| 4 | $\sum_{ijkl} g_{ij}a_{ik}a_{kl} = 0$ | $\mathbf{b}^T\mathbf{A}^2\mathbf{c} + \mathbf{b}^T(\mathbf{c}.\mathbf{Ac}) = \mathbf{b}^T\mathbf{Ac}$ |
| | $\sum_{ijkl} g_{ij}a_{ik}a_{jl} = 0$ | $\mathbf{b}^T(\mathbf{c}.\mathbf{Ac}) = \frac{1}{2}(\mathbf{b}^T\mathbf{c})^2$ |
| 5 | $\sum_{ijklm} g_{ij}a_{jk}a_{kl}a_{lm} = 0$ | $\mathbf{b}^T\mathbf{A}^3\mathbf{c} + \mathbf{b}^T(\mathbf{c}.\mathbf{A}^2\mathbf{c}) = \mathbf{b}^T\mathbf{A}^2\mathbf{c}$ |
| | $\sum_{ijklm} g_{ij}a_{jk}a_{kl}a_{km} = 0$ | $\mathbf{b}^T\mathbf{A}^2\mathbf{c}^2 + \mathbf{b}^T(\mathbf{c}.\mathbf{Ac}^2) = \mathbf{b}^T\mathbf{Ac}^2$ |
| | $\sum_{ijklm} g_{ij}a_{jk}a_{kl}a_{jm} = 0$ | $\mathbf{b}^T\mathbf{A}(\mathbf{c}.\mathbf{Ac}) + \mathbf{b}^T(\mathbf{c}^2.\mathbf{Ac}) = \mathbf{b}^T(\mathbf{c}.\mathbf{Ac})$ |
| | $\sum_{ijklm} g_{ij}a_{jk}a_{kl}a_{im} = 0$ | $\mathbf{b}^T(\mathbf{c}.\mathbf{A}^2\mathbf{c}) + \mathbf{b}^T(\mathbf{Ac})^2 = (\mathbf{b}^T\mathbf{c})(\mathbf{b}^T\mathbf{Ac})$ |
| | $\sum_{ijklm} g_{ij}a_{ik}a_{jl}a_{jm} = 0$ | $\mathbf{b}^T(\mathbf{c}.\mathbf{Ac}^2) + \mathbf{b}^T(\mathbf{c}^2.\mathbf{Ac}) = (\mathbf{b}^T\mathbf{c}^2)(\mathbf{b}^T\mathbf{c})$ |

### 3.2. Pseudo-symplectic Runge–Kutta methods

In this section, pseudo-symplectic RK methods are presented. The classical order conditions are coupled to the pseudo-symplectic equations to yield methods with enhanced energy-conservation properties, compatible with the $s(s+1)/2$ degrees of freedom given by a $s$-stage RK scheme. The resulting schemes are labeled by a synthetic notation indicating the orders of accuracy on solution $p$, on energy conservation $q$ as well as the number of stages (in brackets), e.g., a 2p4q(3) is a three-stage method with second-order accuracy on solution and fourth-order accuracy on energy conservation. Particular attention will be paid to the stability properties of the methods on the imaginary axis (A-stability), that is a fundamental requirement for convection-dominated problems.

#### 3.2.1. 2-stage schemes

Second-order, 2-stage schemes constitute a one-parameter family with $a_{21} = 1/(2b_2)$ and $b_1 = 1 - b_2$. Although no third order can be obtained for the solution ($p = 3$), the remaining parameter can be exploited to achieve $q = 3$, yielding $\theta = 1/2$. The resulting scheme is the well-known improved Euler method (also known as Heun's method or RK2), which is found to be third order on energy conservation, i.e., a 2p3q(2) scheme. To the authors' knowledge, this result has not yet been reported in the existing literature.

#### 3.2.2. 3-stage schemes

Three-stage schemes have 6 free parameters available. Hence, one could in principle look for 3p4q(3) schemes, by coupling the two pseudo-symplectic conditions required for $q = 4$ to the four equations needed to achieve $p = 3$. However, it is easy to verify that none of the existing families of third-order, three-stage schemes (reported e.g., in [18]) satisfy the fourth-order pseudo-symplectic conditions.

On the other hand, one can sacrifice the classical order to obtain enhanced energy conservation properties. For instance, all the Runge–Kutta methods of the type 2p4q(3) have been derived in [7] (labeled as order (2,4) methods, p. 452); however, such schemes are linearly unstable for any value of the free parameter and are thus not suitable for convection-dominated problems.

#### 3.2.3. 4-stage schemes

Four-stage schemes provide 10 degrees of freedom. Usually, these are saturated by enforcing fourth-order accuracy on solution (eight equations). The resulting one- or two-parameter families are available in classical books [18]. It is found that none of the remaining parameters can be adjusted to achieve higher pseudo-symplectic order. As in the case of three-stage schemes, one can lower the classical order of accuracy and seek for 3p5q(4) schemes. The system of equations can be constructed by coupling the 4 classical order conditions to the additional 7 pseudo-symplectic conditions required to achieve fifth-order accuracy on energy conservation. It is easy to verify that two of these 11 equations are dependent upon the others, and therefore the final system has the following 9 independent equations

$$p = 3, q = 3 \begin{cases} \mathbf{b}^T\mathbf{e} = 1 \\ \mathbf{b}^T\mathbf{c} = 1/2 \\ \mathbf{b}^T\mathbf{c}^2 = 1/3 \\ \mathbf{b}^T\mathbf{Ac} = 1/6 \end{cases} \cap \quad q = 5 \begin{cases} \mathbf{b}^T(\mathbf{c}.\mathbf{Ac}) = 1/8 \\ \mathbf{b}^T(\mathbf{Ac})^2 = 1/24 \\ \mathbf{b}^T\left(\mathbf{c}.\mathbf{Ac}^2\right) + \mathbf{b}^T\left(\mathbf{c}^2.\mathbf{Ac}\right) = 1/6 \\ \mathbf{b}^T\mathbf{A}^2\mathbf{c} = 1/24 \\ \mathbf{b}^T\left(\mathbf{c}.\mathbf{A}^2\mathbf{c}\right) = 1/24 \end{cases}, \tag{14}$$

and can be solved by means of a symbolic nonlinear solver. The result is a new one-parameter family:

**Table 2**
Summary of pseudo-symplectic methods.

| Method | Source | $s$ | $p$ | $q$ | $\sigma_i$ | Notation |
|---|---|---|---|---|---|---|
| Improved Euler | [19], p. 129 | 2 | 2 | 3 | 0 | 2p3q(2) |
| Order (4,2) | [7], p. 452 | 3 | 2 | 4 | 0 | 2p4q(3) |
| 3p5q(4) | Section 3.2.3 | 4 | 3 | 5 | 2.85 | 3p5q(4) |
| PS63 | [7], p. 453 | 5 | 3 | 6 | 2.85 | 3p6q(5) |
| 4p7q(6) | Section 3.2.4 | 6 | 4 | 7 | 3.71 | 4p7q(6) |

3p5q(4)

$$
\begin{array}{c|cccc}
0 & 0 & & & \\
\frac{c_3-1}{4c_3-3} & \frac{c_3-1}{4c_3-3} & 0 & & \\
c_3 & c_3-\frac{(2c_3-1)(4c_3-3)}{2(c_3-1)} & \frac{(2c_3-1)(4c_3-3)}{2(c_3-1)} & 0 & \\
1 & -\frac{(2c_3-1)^2}{2(c_3-1)(4c_3-3)} & \frac{6c_3^2-8c_3+3}{2(c_3-1)(2c_3-1)} & \frac{c_3-1}{(2c_3-1)(4c_3-3)} & 0 \\
\hline
 & \frac{1}{12(c_3-1)} & \frac{(4c_3-3)^2}{12(c_3-1)(2c_3-1)} & -\frac{1}{12(c_3-1)(2c_3-1)} & \frac{4c_3-3}{12(c_3-1)}
\end{array}
,
$$

with $c_3 \neq \{1/2, 3/4, 1\}$, and $c_3 \in ]0, 3/4[ \cup ]1, +\infty[$ to have positive $c_i$ coefficients. In what follows, the baseline $3p5q(4)$ scheme is computed by choosing $c_3 = 1/4$, that leads to a Butcher tableau of simple rational numbers.

*3.2.4. Higher-order schemes*

A systematic derivation for a number of stages higher than 4 becomes significantly involved and has not been attempted here. A particularly promising scheme is the five-stage method developed in [7] (labeled as PS63, p. 453), which is of the type 3p6q(5). In the same work, it was also demonstrated that no 4p8q(6) methods exist. Subsequently, a 4p7q(6) one-parameter family was obtained by Calvo et al. [8]. In order to apply the method to the Navier–Stokes equations, the family derived in [8] has been optimized to take into account stability and minimization of the coefficients of the principal term of the local error, yielding the following new method:

4p7q(6)

$$
\begin{aligned}
a_{21} &= 0.23593376536651968050;\ a_{31} = 0.347507356584235168;\ a_{32} = -0.135619353983464433;\\
a_{41} &= -0.20592852403227;\ a_{42} = 1.891790766221084;\ a_{43} = -0.89775024478958;\\
a_{51} &= -0.094354932814554;\ a_{52} = 1.756171412237619;\ a_{53} = -0.967078504769475;\\
a_{54} &= 0.069328259979890148;\ a_{61} = 0.14157883255197;\ a_{62} = -1.17039696277833;\\
a_{63} &= 1.30579112376331;\ a_{64} = -2.203541368552894;\ a_{65} = 2.9265683750159476;\\
b_1 &= b_6 = 0.07078941627598264;\ b_2 = b_5 = 0.87808570611880957;\ b_3 = b_4 = -0.448875122394792210.
\end{aligned}
$$

*3.2.5. Summary of pseudo-symplectic methods*

The existing as well as the newly derived pseudo-symplectic methods are summarized in Table 2. The intersection of the linear stability footprint of each method with the imaginary axis, $\sigma_i$, is also reported in Table 2. Time integration of convection-dominated flows requires $\sigma_i > 0$. Therefore, only the last three schemes are selected for application to the Navier–Stokes equations, and will be tested numerically in the next section. It is worth to remark that strictly positive Butcher arrays are not required because of the smoothness of incompressible Navier–Stokes solutions [9].

## 4. Numerical results

In this section, the performances of pseudo-symplectic as well as classical RK schemes are assessed and compared. A summary of the methods used in numerical tests is given in Table 3, along with the symbols that will be used to denote each scheme in the figures.

In all tests, spatial discretization is achieved by means of a standard pseudo-spectral method [20], with the convective term discretized in skew-symmetric form, yielding a spatially energy-conserving scheme [21]. For the symplectic Gauss scheme, the implicit system is solved by a fixed-point iterative algorithm to machine accuracy. For classical and pseudo-symplectic methods, the only energy-conservation error provided by the overall method is due to the time-integration scheme. It is worth to remind that the maximum CFL number dictated by linear stability is equal to $\sigma_i / w_m$, where $\sigma_i$ is given in Table 2 and $w_m = \pi$ for spectral differentiation [22].

**Table 3**
Summary of Runge–Kutta methods used in numerical tests.

| Method | $s$ | $p$ | $q$ | $\sigma_i$ | Notation | Symbol |
|---|---|---|---|---|---|---|
| Gauss [16] | 1 | 2 | Symplectic | A-stable | 2p(1) | — |
| Kutta's rule [19] | 3 | 3 | 3 | $\sqrt{3}$ | 3p3q(3) | ○ |
| RK4 [19] | 4 | 4 | 4 | 2.85 | 4p4q(4) | □ |
| 3p5q(4) | 4 | 3 | 5 | 2.85 | 3p5q(4) | ▲ |
| PS63 [7] | 5 | 3 | 6 | 2.85 | 3p6q(5) | ♦ |
| 4p7q(6) | 6 | 4 | 7 | 3.71 | 4p7q(6) | ▶ |

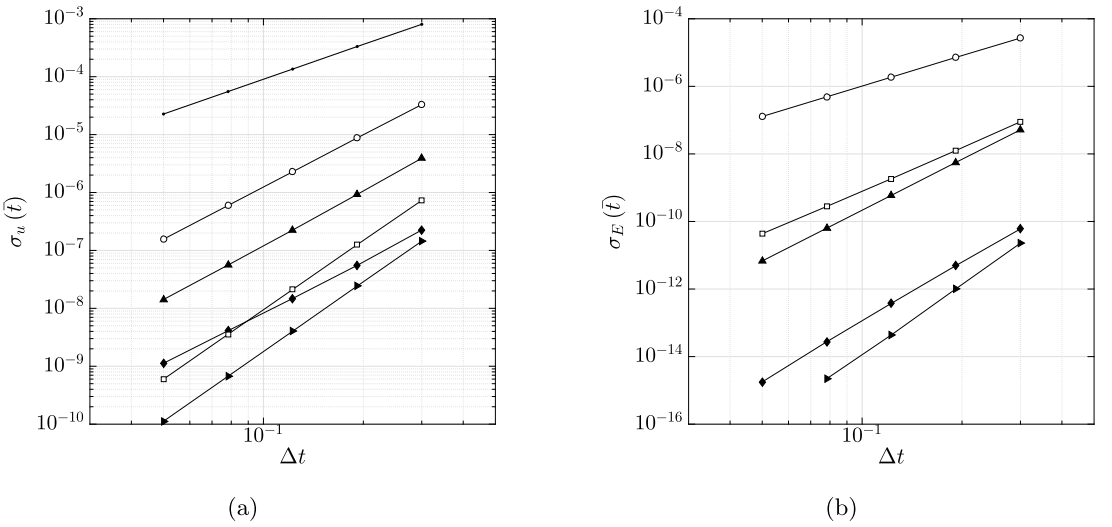


**Fig. 1.** Results for the inviscid random flow, with $\bar{t} = 5$. (a) Order of accuracy on solution. (b) Order of accuracy on energy conservation. Symbols are defined in Table 3.

### 4.1. Order of accuracy study

The aim of the first test is to verify that the predicted orders of accuracy on solution and on energy conservation are actually obtained numerically, so that the correctness of the theoretical framework is confirmed. To this end, a two-dimensional, inviscid periodic random flow is considered, similarly as done in [3]. Being free of any symmetry, this test is very effective in showing the true order of accuracy of a method, since any fortuitous error cancellation is avoided. Since viscous dissipation is not taken into account, and the spatial discretization is discretely energy conserving, it is expected that energy is either conserved to machine accuracy (for symplectic schemes) or to $\mathcal{O}(\Delta t^q)$ (for pseudo-symplectic ones). A divergence-free initial velocity field is constructed from a stream function of random numbers, and advanced in time on a square region of size $2\pi L \times 2\pi L$, discretized on $16 \times 16$ mesh points. The initial flowfield is normalized such that $u$ and $v$ have zero mean, and $E_0 = 1.0$. In the following, time is expressed in units of $L/\sqrt{E_0}$.

Simulations have been carried out at time steps $\Delta t \in [0.05, 0.3]$, corresponding to CFL numbers lying (roughly) in the interval $[0.02, 0.1]$, hence well within the linear stability region of each scheme. The following normalized error measures are defined

$$\sigma_u(t) = \frac{\|\mathbf{u}_x(t) - \mathbf{u}_x(t)_{\Delta t \to 0}\|_2}{\|\mathbf{u}_x(t)_{\Delta t \to 0}\|_2}, \quad \sigma_E(t) = \left| \frac{E(t) - E_0}{E_0} \right|. \tag{15}$$

In the following, the errors are measured at $t = \bar{t} = 5$. Note that the error for $u$ is computed by taking as a reference a numerical solution obtained using a very small time step ($5 \times 10^{-4}$).

Results are shown in Fig. 1. Both graphs fully confirm the theoretical orders of accuracy on solution and on energy conservation for all methods. In particular, Fig. 1(a) shows that, on equal order of accuracy, the pseudo-symplectic schemes have much lower errors $\sigma_u$ with respect to standard RK3 and RK4. The 3p6q(5) method performs even better than the RK4 in a specific range of $\Delta t$ considered. Although no definitive conclusions can be deduced from this analysis, it appears that pseudo-symplectic methods have small error constants, thus partially compensating the fact that their classical order of accuracy has not been maximized. On the other hand, it is worth to remark that the 3p6q(5) and 4p7q(6) methods require one and two additional stages, respectively, with respect to the RK4 scheme. Similar considerations can be drawn from Fig. 1(b). The error levels of the pseudo-symplectic schemes are significantly lower than those of standard ones in the whole range of $\Delta t$ considered. The order on energy conservation for the Gauss scheme is not shown since its error is null to machine accuracy for every $\Delta t$.

### 4.2. Three-dimensional Taylor–Green vortex

The energy-conservation properties of the proposed schemes are studied in a more physical context by simulating the three-dimensional Taylor–Green vortex at high Reynolds number. In this case, the initial distribution of vorticity is subject to vortex stretching, thus generating smaller scales and eventually leading to transition to turbulence and subsequent decay [23].

The initial condition is given as

$$\begin{aligned} u(x,y,z,0) &= U_0 \frac{2}{\sqrt{3}} \sin(\theta + \frac{2}{3}\pi) \sin(x) \cos(y) \cos(z), \\ v(x,y,z,0) &= U_0 \frac{2}{\sqrt{3}} \sin(\theta - \frac{2}{3}\pi) \cos(x) \sin(y) \cos(z), \\ w(x,y,z,0) &= U_0 \frac{2}{\sqrt{3}} \sin(\theta) \cos(x) \cos(y) \sin(z), \end{aligned} \tag{16}$$

with $\theta = 0$. Starting from Eqs. (16), the incompressible Navier–Stokes equations are advanced in time in a tri-periodic cube of side $2\pi L$. The problem is entirely governed by the Reynolds number Re (based on $L$ and $U_0$). Two values will be considered in the following: $\mathrm{Re} = 1600$ and $\mathrm{Re} = 3000$, both are chosen to be sufficiently high to trigger transition to turbulence, that occurs around $t = 9$ (in units of $L/U_0$). A computational mesh of $64^3$ points is chosen. This is a typical resolution for LES [24]; however, no subgrid-scale model is employed in this work, in order to effectively isolate the numerical errors coming from the temporal scheme. The interaction of the numerical error with a subgrid-scale model will not be taken into consideration here.

Clearly, for this test kinetic energy is not conserved due to (physical) viscous dissipation. An ideal numerical method should thus ensure that the energy decay is exclusively provided by the scalar dissipation function, cfr. Eq. (10). When this balance is not discretely enforced, numerical diffusion (or anti-diffusion) can compete with molecular viscosity (or turbulence models, if any) and alter the underlying physics of the flowfield. As an adequate parameter to quantify these effects, the *effective* Reynolds number $\mathrm{Re}^*$ is introduced, defined as

$$\mathrm{Re}^{*,n+1} \equiv \frac{\overline{\Phi}}{(E^{n+1} - E^n)/\Delta t}, \tag{17}$$

where $\overline{\Phi}$ is the mean integral value of the discrete scalar dissipation function, determining the variation of energy between two consecutive time-steps $n$ and $n+1$,

$$\overline{\Phi} \equiv \sum_i b_i \mathbf{u}_i^T \mathbf{L}\mathbf{u}_i. \tag{18}$$

The definitions given in Eq. (17) and Eq. (18) deserve further comments. With reference to the discrete energy balance Eq. (9), note that the effective Reynolds number quantifies the magnitude of the spurious temporal error with respect to the physical viscous dissipation term. For symplectic methods, $\mathrm{Re}^* = \mathrm{Re}$ at all time steps, while $|1 - \mathrm{Re}^*/\mathrm{Re}| = \mathcal{O}\left(\Delta t^q\right)$ for pseudo-symplectic schemes (and for finite Re). This property is independent of the classical temporal order as well as of the spatial discretization, although $\overline{\Phi}$ is clearly a fully discrete (spatial and temporal) approximation of its *exact* counterpart, i.e., $\frac{1}{\Delta t}\int_t^{t+\Delta t} \phi \, dt$, cfr. Eq. (10). The discrete scalar dissipation function can be easily computed during the simulation by evaluating the quantity $\mathbf{u}_i^T \mathbf{L}\mathbf{u}_i$ at each RK stage.

Results are shown in Fig. 2. The ratio of the effective Reynolds number to the nominal Reynolds number is shown for the two cases $\mathrm{Re} = 1600$ and $\mathrm{Re} = 3000$, both performed at CFL = 0.5. It is expected that as the Reynolds number increases, the viscous dissipation term and the temporal error can become of comparable magnitude. Firstly, note that $\mathrm{Re}^*/\mathrm{Re} \leq 1$ for all schemes and at all times; therefore, all methods turn out to be (at most) dissipative and hence no anti-diffusion occurs. However, the RK3 and RK4 schemes show significant deviations from unity. In particular, for the $\mathrm{Re} = 3000$ case, the effective Reynolds numbers of the RK3 and RK4 methods drop to $\approx 2820$ and $\approx 2970$, respectively, at the peak of the dissipation rate, that approximately equals the time of transition to turbulence. Therefore, the solver is spuriously adding artificial viscosity to the solution and altering the physical realism of the simulation by modifying the governing parameter of the flow. On the contrary, the pseudo-symplectic methods perform remarkably well, especially the higher-order ones, namely 3p6q(5) and 4p7q(6), although 1 and 2 additional sub-stages are required, respectively, in comparison with the standard RK4. For such methods, the relative error is always lower than $4 \times 10^{-4}$, as shown in the inset plot of Fig. 2. On the other hand, the 3p5q(4) and the RK4 provide similar results. The symplectic Gauss method keeps the nominal Reynolds number (to machine accuracy) throughout the entire simulation. Tests at different grid resolutions (not shown here) confirm the same trends of Fig. 2.

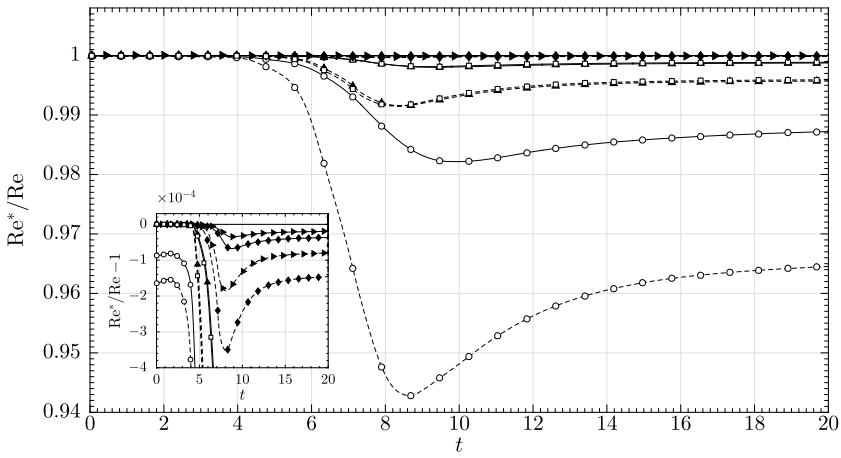


**Fig. 2.** Ratio of effective to nominal Reynolds number for $\mathrm{Re} = 1600$ (solid line) and $\mathrm{Re} = 3000$ (dashed line) as a function of time for the various schemes listed in Table 3. The inset plot shows an enlarged view of the error for the best pseudo-symplectic methods.

## 5. Conclusions

Pseudo-symplectic Runge–Kutta methods for time-integration of the incompressible Navier–Stokes equations have been investigated. The use of explicit time-stepping schemes with optimal energy-conservation properties is particularly appealing, since algorithms that preserve kinetic energy in time exactly are necessarily implicit and might be not applicable in practical situations. A survey of existing and newly derived pseudo-symplectic methods has led to the selection of three schemes with prescribed orders of accuracy on solution and energy conservation.

Numerical results have confirmed the theoretical predictions and have shown that the pseudo-symplectic schemes can provide much lower energy-conservation errors than classical ones. Also, it has been found that the proposed methods have small error constants, despite the fact that the maximum order of accuracy achievable has been sacrificed to enhance their energy-conservation properties.

In viscous simulations, it has been shown that at high Reynolds numbers the error on energy variation can become comparable to the viscous dissipation rate. This effect has been quantified upon introduction of an effective Reynolds number (taking into account both physical and artificial viscosity) that, for standard schemes, can be significantly different from the nominal one. On the contrary, pseudo-symplectic methods are able to minimize such discrepancies.

A promising field of application for pseudo-symplectic schemes is the numerical simulation of turbulent flows. The need for computational efficiency and energy-conservation properties makes them ideal candidates in LES or DNS computations.

## References

[1] C. Foias, O. Manley, R. Rosa, R. Temam, Navier–Stokes Equations and Turbulence, Cambridge University Press, 2004.
[2] J.B. Perot, Discrete conservation properties of unstructured mesh schemes, Annu. Rev. Fluid Mech. 43 (2011) 299–318.
[3] F. Capuano, G. Coppola, G. Balarac, L. de Luca, Energy preserving turbulent simulations at a reduced computational cost, J. Comput. Phys. 298 (2015) 480–494.
[4] A. Palha, M. Gerritsma, A mass, energy, enstrophy and vorticity conserving (MEEVC) mimetic spectral element discretization for the 2D incompressible Navier–Stokes equations, J. Comput. Phys. (2016), http://dx.doi.org/10.1016/j.jcp.2016.10.009.
[5] F. Capuano, G. Coppola, L. de Luca, An efficient time advancing strategy for energy-preserving simulations, J. Comput. Phys. 295 (2015) 209–229.
[6] E. Hairer, C. Lubich, G. Wanner, Geometric Numerical Integration, Springer, 2006.
[7] A. Aubry, P. Chartier, Pseudo-symplectic Runge–Kutta methods, BIT Numer. Math. 38 (1998) 439–461.
[8] M. Calvo, M. Laburta, J. Montijano, L. Rández, Approximate preservation of quadratic first integrals by explicit Runge–Kutta methods, Adv. Comput. Math. 32 (2010) 255–274.
[9] B. Sanderse, B. Koren, Accuracy analysis of explicit Runge–Kutta methods applied to the incompressible Navier–Stokes equations, J. Comput. Phys. 231 (2012) 3041–3063.
[10] Y. Morinishi, T.S. Lund, O.V. Vasilyev, P. Moin, Fully conservative higher order finite difference schemes for incompressible flows, J. Comput. Phys. 143 (1998) 90–124.
[11] F. Felten, T. Lund, Kinetic energy conservation issues associated with the collocated mesh scheme for incompressible flow, J. Comput. Phys. 215 (2006) 465–484.
[12] R.W.C.P. Verstappen, A.E.P. Veldman, Symmetry-preserving discretization of turbulent flow, J. Comput. Phys. 187 (2003) 343–368.
[13] A.G. Kravhcenko, P. Moin, On the effect of numerical errors in large eddy simulations of turbulent flows, J. Comput. Phys. 131 (1997) 310–322.
[14] F. Harlow, J. Welch, Numerical calculation of time-dependent viscous incompressible flow of fluid with free surface, Phys. Fluids 8 (1965) 2182–2189.
[15] J. Rosenbaum, Conservation properties of numerical integration methods for systems of ordinary differential equations, J. Comput. Phys. 20 (1976) 259–267.
[16] B. Sanderse, Energy-conserving Runge–Kutta methods for the incompressible Navier–Stokes equations, J. Comput. Phys. 233 (2013) 100–131.
[17] J.M. Sanz-Serna, Runge–Kutta schemes for Hamiltonian systems, BIT Numer. Math. 28 (1988) 877–883.
[18] J.C. Butcher, Numerical Methods for Ordinary Differential Equations, Wiley, 2004.

[19] D.F. Griffiths, D.J. Higham, Numerical Methods for Ordinary Differential Equations, Springer, 2010.
[20] C. Canuto, M. Hussaini, A. Quarteroni, T. Zang, Spectral Methods. Evolution to Complex Geometries and Applications to Fluid Dynamics, Springer, 2007.
[21] F. Capuano, G. Coppola, M. Chiatto, L. de Luca, Approximate projection method for the incompressible Navier-Stokes equations, AIAA J. 54 (2016) 2179–2182.
[22] S.K. Lele, Compact finite difference schemes with spectral-like resolution, J. Comput. Phys. 103 (1992) 16–42.
[23] M.E. Brachet, D.I. Meiron, S.A. Orszag, B.G. Nickel, R.H. Morf, U. Frisch, Small-scale structure of the Taylor–Green vortex, J. Fluid Mech. 130 (1983) 411–452.
[24] G.J. Gassner, A.D. Beck, On the accuracy of high-order discretizations for underresolved turbulence simulations, Theor. Comput. Fluid Dyn. 27 (2013) 221–237.